THE HETEROGENEOUS MANTLE UNDER SOUTH POLE-AITKEN BASIN AS CONSTRAINED BY GRAIL AND LOLA OBSERVATIONS.

Peter B. James[1], David E. Smith[2], Jordan D. Kendall[3], Maria T. Zuber[2], Sean C. Solomon[1], [1]Lamont-Doherty Earth Observatory, Columbia University, Palisades, NY 10901 (pjames@alum.mit.edu). [2]Department of Earth, Atmospheric and Planetary Sciences, Massachusetts Institute of Technology, Cambridge, MA 02139. [3]Department of Physics, Purdue University, West Lafayette, IN 47907.

Background: The South Pole-Aitken (SP-A) basin is by far the largest preserved impact structure on the Moon, with a major axis of 2400 km and a minor axis of 2050 km [1]. Constraints on the structure of the mantle under SP-A provide important information for modeling the basin-forming impact event as well as the subsequent chemical evolution of the lunar interior. In particular, it has been suggested that a large oblique impact may have produced up-range/down-range asymmetry in the structure of mantle rebound [2].

Data from the Gravity Recovery and Interior Laboratory (GRAIL) mission [3] along with topographic measurements from the Lunar Orbiter Laser Altimeter (LOLA) [4] allow us to probe the mantle under SP-A. Interpretation of the Moon's deep structure is complicated by the inherent ambiguity associated with gravity/topography analyses; the gravity signal associated with deep anomalies can be obscured by shallow anomalies even at the longest wavelengths. A previous forward modeling study yielded some mantle anomalies that approximately reproduce the Bouguer gravity anomaly at SP-A [5], but at least some of the gravity signal likely arises from crust-mantle interface relief.

In this analysis, we isolate the mantle gravity signature through a combination of spectral filtering and best-fit determination. We perform an analysis of topography/geoid power and cross-power spectra to calculate the best-fit geoid-to-topography ratio (*GTR*) associated with sub-crustal mass anomalies. We use the *GTR*s to infer the characteristic depth of mass anomalies in the mantle. We then determine the lateral variations in the mantle under most of the SP-A basin interior with a two-layered inversion.

Constraining the Mantle Anomaly Depth: Observed topography may be expressed as superpositions of two or more components. In this study, we define H_c to be the portion of topography corresponding to shallow compensation and H_d to be the remaining portion broadly associated with deep-seated compensation and/or elastic support. The power and cross-power spectra of these topographic components may then be related to the observed spectra:

$$\begin{bmatrix} S_{HH} \\ S_{NN} \\ S_{HN} \end{bmatrix} = \begin{bmatrix} 1 & 1 & 2 \\ GTR_c^2 & GTR_d^2 & 2GTR_cGTR_d \\ GTR_c & GTR_d & GTR_c+GTR_d \end{bmatrix} \begin{bmatrix} S_{H_cH_c} \\ S_{H_dH_d} \\ S_{H_cH_d} \end{bmatrix} \quad (1)$$

where N is the geoid, and S denotes power, i.e., the expected amplitude of the product in the subscript. If GTR_c (the *GTR* associated with H_c) is known *a priori*, the system of equations has four unknowns: GTR_d (the *GTR* associated with H_d) and the three terms on the right-hand side of equation (1).

If deep topography and crustal topography are uncorrelated (i.e., their cross-power spectrum $S_{H_cH_d}$ is zero), GTR_d may then be determined from the observed power and cross-power spectra of topography and gravity:

$$GTR_d = \frac{S_{NN} - GTR_c S_{HN}}{S_{HN} - GTR_c S_{HH}} \quad (2)$$

Coincidentally, this is the value of GTR_d that minimizes the power of shallowly compensated topography, $S_{H_cH_c}$. More generally, we can define a correlation factor $r = S_{H_cH_d} / \sqrt{S_{H_cH_c}S_{H_dH_d}}$ and solve for the value of GTR_d associated with an arbitrary r. A negative value of r indicates that thin crust is correlated with a deficit of mass in the mantle, and vice versa.

Compensation Depth: The *GTR* associated with dynamic compensation of topography as a function of loading depth d_m may be calculated as a spectrally weighted sum of the dynamic admittance kernel Z_l, which is a function of spherical harmonic degree l:

$$GTR_d = \sum_{l=3}^{l_{max}} (V_l Z_l) \Big/ \sum_{l=3}^{l_{max}} V_l \quad (3)$$

where V_l denotes the topographic power spectrum [6,7]. We use the global lunar topographic power as an approximation for the spectrum V_l within SP-A. GTR_d is an injective and non-surjective function of the compensation depth d_m, so a limited range of GTR_d values inferred via equation (1) may be used to determine d_m.

Results: In order to calculate power and cross-power spectra, we sampled topography and the geoid on an icosahedral grid. Data points within a tapered SP-A boundary were retained, and data inside Apollo basin were excluded.

*GTR*s associated with deep compensation of topography are given in Table 1 along with the inferred anomaly depth d_m. A plot of geoid versus topography is shown in Figure 1 along with the slopes for GTR_c, GTR_d (for $r = 0$), and the observed *GTR*. We assumed $GTR_c = 5$ m/km, as this value provided a good fit to the short-wavelength slopes in geoid/topography. The value of GTR_d can be larger or smaller than the ob-

served *GTR* depending on the value of *r*. The assumption of zero correlation between H_c and H_d corresponds to a depth $d_m \cong 500$ km. The anomaly depth varies considerably for non-zero values of *r,* but a lower bound on d_m is better constrained than an upper bound.

Table 1 – Observed *GTR* and gravity/topography correlation γ in SP-A, along with GTR_d and d_m inferred for several values of *r*.

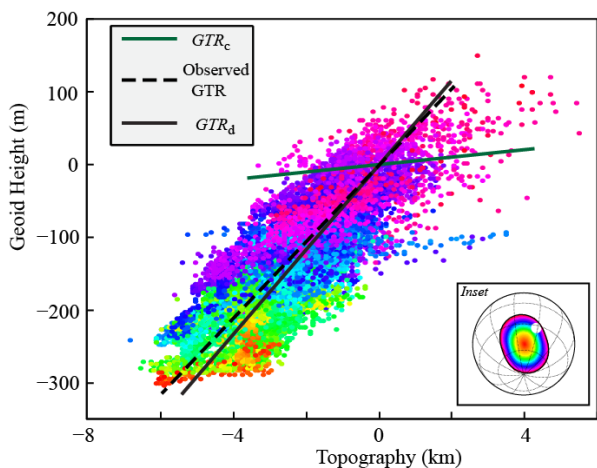| *r*	Obs. *GTR* (m/km)	γ	GTR_d (m/km)	d_m (km)
0.2			61.2	>1500
0.1			59.1	858
0			57.3	537
-0.1	51.8	0.956	55.6	435
-0.2			53.9	372
-0.3			52.3	325
-0.4			50.6	287
-0.5			48.7	254

Figure 1. Geoid height versus topography inside SP-A (excluding Apollo basin). The value of GTR_c, observed best-fit slope, and GTR_d are represented by the slopes of the straight lines. Colors indicate location within SP-A (see inset).

We use this anomaly depth d_m to perform a two-layered inversion of gravity and topography. We tapered gravity and topography to the interior of the basin and applied a low-pass filter to the mantle anomaly such that the power spectrum is proportional to l^2 above $l=8$. The mantle anomaly is plotted in Figure 2.

Whenever gravity and topography are used to infer mantle anomalies, one must carefully consider the possibility of elastic support. Since certain configurations of elastic loading produce *GTR*s comparable to those of deep-seated dynamic topography, it can be easy for one to masquerade as the other. In particular, the mascon at the Apollo basin is associated with an apparent

mantle anomaly (masked out in Figure 2). However, the remaining mass anomalies do not appear to correlate strongly with impact basins. If it exists, any significant elastic support of topography likely results from volcanic loading rather than impact processes.
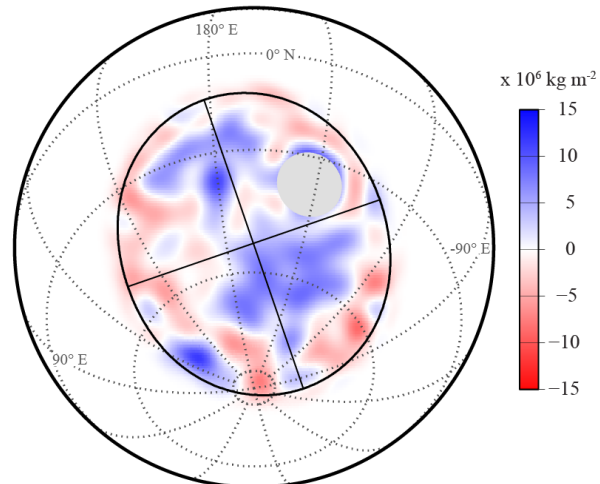

Figure 2 – Mantle mass anomaly, tapered to the interior of the SP-A basin (black ellipse with semi-major and semi-minor axes) and spectrally filtered with a critical degree $l_c=20$. The Apollo basin is masked out.

Conclusions: A considerable portion of the SP-A basin interior appears to be associated with a positive mass anomaly in the mantle. The anomaly amplitudes shown in Figure 2 could be reproduced by ±50 km of relief on an interface with a 200 kg m^{-3} density contrast, or alternatively by ±1% density variations distributed over ~300 km depth. These amplitudes decrease if the inferred anomaly depth d_m is shallower.

The mantle anomaly pattern is somewhat symmetric about the major axis of the basin and asymmetric about the minor axis. The best-fit depth of the mantle anomaly is ~500 km for $r=0$, but for a parameter range of -0.5 < *r* < 0.2, the inferred value of GTR_d may be compatible with any depth d_m greater than ~250 km. This anomaly depth should be understood as a single representative depth which, in reality, likely corresponds to the superposition of a variety of anomalies at depths throughout the lunar mantle.

References: [1] Garrick-Bethell I. and Zuber M. T. (2009) *Icarus 204*, 399-408. [2] Elbeshausen D. et al. (2009) *Icarus 204*, 716-731. [3] Zuber M. T. et al. (2013) *Science 339*, 668-671. [4] Smith D. E. et al. (2010) *Geophys. Res. Lett. 37*, L18204. [5] Smith D. E. et al. (2014) *LPS 45*, abstract 1956. [6] Hager B. H. et al. (1985) *Nature 313,* 541-545. [7] Wieczorek M. A. and Phillips R. J. (1997) *J. Geophys. Res. 102*, 10,933-10,943.